Draft version December 14, 2023
Typeset using LaTeX **twocolumn** style in AASTeX631

Constraining Explosion Model Parameters for Supernova 1987A Through Analysis of Photon Light Curves*

Levi Webb,[1] Brandon Barker,[1,2,3,4,5,†] Erin Syerson,[1] and Sean Couch[1,2,6]

[1] *Department of Physics and Astronomy, Michigan State University, East Lansing, MI 48824, USA*
[2] *Department of Computational Mathematics, Science, and Engineering, Michigan State University, East Lansing, MI 48824, US*
[3] *Computational Physics and Methods, Los Alamos National Laboratory, Los Alamos, NM 87545, USA*
[4] *Center for Nonlinear Studies, Los Alamos National Laboratory, Los Alamos, NM 87545, USA*
[5] *Center for Theoretical Astrophysics, Los Alamos National Laboratory, Los Alamos, NM 87545, USA*
[6] *Facility for Rare Isotope Beams, Michigan State University, East Lansing, MI 48824, USA*

ABSTRACT

Current simulations of core-collapse supernova (CCSN) explosions are not able to unambiguously reproduce observed light curves from Type II SNe. In order to address this problem and better understand the mechanisms of SN explosions and their progenitors, we present new models of SN 1987A based on a physically accurate explosion model using realistic initial conditions. We use a state-of-the-art 1D code for neutrino-driven CCSNe, SN Turbulence In Reduced-dimensionality (STIR; Couch et al. 2020), to simulate stellar core collapse and explosion in blue supergiant progenitors from Menon & Heger (2017). Using output data from STIR, we generate model bolometric light curves with the SN Explosion Code (SNEC; Morozova et al. 2015). We model neutrino emission with SN Observatories with GLoBES (SNOwGLoBES; Migenda) to predict observable neutrino count rates and spectra. The results from SNEC and SNOwGLoBeS are compared to existing observational data of SN 1987A to assess the ability of our numerical models to match the actual observations of SN 1987A. We also compare our results to existing models of SN 1987A and other SNe.

1. INTRODUCTION

When a massive star reaches the end of its life, it dies in a radiant supernova (SN). Sufficiently massive stars—with a zero-age main sequence mass of $\gtrsim 8M_\odot$ (Branch & Wheeler 2017)—form an iron core that eventually succumbs to gravitational collapse, releasing incredible amounts of energy and heavy elements in the form of core-collapse supernovae (CCSNe). Current understandings of CCSNe assert that this process is driven by neutrino heating (Bethe & Wilson 1985; Nadyozhin & Imshennik 2005; Couch & Ott 2015).

Existing 3D models of CCSNe are computationally expensive and, as such, are rarely simulated. While unable to reproduce the depth of 3D models, spherically symmetric 1D models offer a relatively inexpensive alternative to studying CCSNe. It has been historically difficult to achieve accurate explosion simulations in 1D due to the importance of convection and turbulence (Couch & Ott 2015); however, a new method for computing CCSNe in 1D has recently been introduced that addresses and applies these issues ("STIR" Couch et al. 2020, see Section 2.2). In this investigation, we use STIR to explore photon emissions of CCSNe from blue supergiant progenitors (stars pre-explosion), aiming to further constrain the parameters of the progenitor of SN 1987A. We pair this with another code ("SNEC" Morozova et al. 2015) to produce photon emissions comparable to observational data (Hamuy et al. 1988) of SN 1987A.

1.1. *Classifications*

The properties of a SN—including its progenitor parameters—are revealed through its energy output (Figure 1). SNe are classified by the presence (Type II) or absence (Type I) of hydrogen lines in their optical spectra at peak brightness (Branch & Wheeler 2017; Minkowski 1941). Type II SNe are further classified by the shape of the plot of their bolometric luminosity as a function of time, or light curve. Most generally, a SN whose luminosity linearly declines after the initial explosion is classified as Type IIL, and those with a plateau in their light curve are Type IIP (Nadyozhin & Imshennik 2005, Figure 1 provides an example of the latter). Typical CCSNe produce Type II light curves.

* Alternatively: The Big Investigation into The Explosion of SN 1987A, or The BITE of '87.

† NSF Fellow

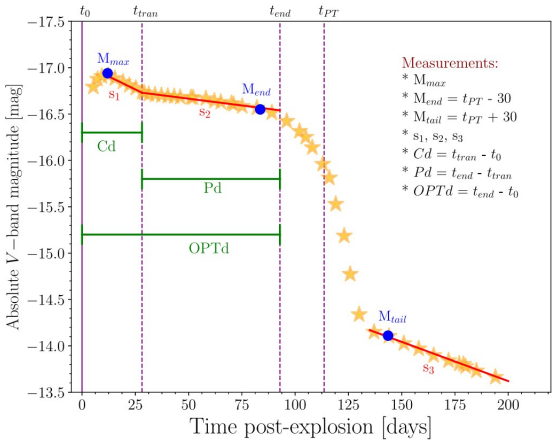

Figure 1. Example from Gutiérrez et al. (2017) of measurable quantities on a Type IIP light curve. Each of these is dependent on progenitor parameters. The blue points reference magnitude values (in our investigation, we instead examine the bolometric luminosity), and the cooling (Cd), plateau (Pd), and optically thick phase (OPTd) durations are shown in green. There are three measurable slopes for this light curve, plotted in red—s_3 is known as the radioactive tail. Gutiérrez et al. (2017) also labels four epochs: the time of explosion (t_0), the transition between s_1 and s_2 (t_{tran}), the end of the optically thick phase (t_{end}), and the midpoint of the transition between plateau and tail.

1.2. *SN 1987A*

SN 1987A took place in the Large Magellanic Cloud (LMC West et al. 1987), making it the closest SN to occur in modern astronomy and an excellent candidate for study. In fact, it is so close that it is the only SN to date with associated neutrino observations (Hirata et al. 1987; Bionta et al. 1987; Raffelt 2011).

Unlike most Type II SNe with red supergiant (RSG) progenitors, SN 1987A is thought to have occurred as a direct result of a blue supergiant (BSG) merger (Menon & Heger 2017). This is indicated by its under-luminous (McCray 1993; Arnett et al. 1989), dome-shaped light curve (Figure 2; Hamuy et al. 1988; Catchpole et al. 1988) and confirmed by analysis of photographic plates of the LMC exposed prior to the explosion (Blanco et al. 1987; Meurer et al. 1987; Menon & Heger 2017).

Due to its odd light curve, SN 1987A is classified as a Type II-Peculiar SN. The goal of the work outlined in this paper is to ascertain the conditions under which SN 1987A produced said light curve.

2. METHODS

2.1. *Progenitors*

For this work, we use progenitor stars from Menon & Heger (2017), as presented in Table 1. These progenitors result from blue supergiant (BSG) binary mergers, and

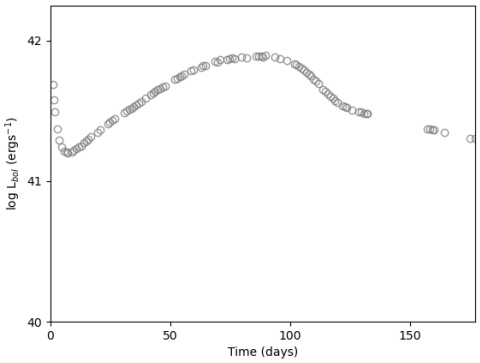

Figure 2. Observational data of SN 1987A plotted from Hamuy et al. (1988). This is also included on each of our light curves and that of Utrobin et al. (2021), to which we compare our work in Figure 6.

Model	M_1 ($M_\odot$)	M_2 ($M_\odot$)	M_{tot} ($M_\odot$)	Explosion Energy (10^{51}ergs)
15-7b	15	7	22	0.777
15-8b	15	8	23	0.458
16-4a	16	4	20	0.734
16-7b	16	7	23	0.446
17-7a	17	7	24	0.832
17-8a	17	8	25	1.085

Table 1. Progenitor model masses from Menon & Heger (2017) and explosion energies as calculated by SNEC for our fiducial runs of the models.

the models are identified by the individual masses of their respective stars.

Menon & Heger (2017) presents merger progenitors rather than single stars of the same total mass. The LMC has sub-solar metallicity, implying a weak line-driven stellar wind (Muijres 2010) and thus a low mass-loss rate, indicative of the merger progenitors we use for this study. A single, high mass progenitor with solar metallicity would have strong winds and a high mass-loss rate—the hydrogen loss from this is enough to make the star blue. However, these light curves would look very different than that of SN 1987A, so we use a merger model to produce a lower mass BSG at the point of core collapse.

2.2. *Computations*

Our computations begin with a 1D neutrino-driven CCSN hydrodynamics code, SN Turbulence In Reduced-dimensionality (STIR; Couch et al. 2020), which simulates spherically symmetric progenitor explosions with detailed high-density microphysics out to a few seconds. Given STIR's treatment of neutrino transport, we ex-

pect that it reliably produces physically accurate explosion energies.

We then pass outputs from STIR into the SN Explosion Code (SNEC; Morozova et al. 2015), a photon radiation hydrodynamics code in the equilibrium diffusion approximation that uses computationally cheaper microphysics to generate bolometric light curves up to and beyond 200 days. The use of a Lagrangian basis allows SNEC to compute light curves to late times for progenitors with very large radii. SNEC also allows us to vary the progenitor parameters and explore how they affect the resultant light curve, providing a greater understanding of the explosion mechanisms of SN 1987A.

3. RESULTS

3.1. *Fiducial Bolometric Light Curves*

We began our investigation with computations by STIR and SNEC with no modifications to the progenitors. We plot the resulting light curve for each model with reference to observational data of SN 1987A (Hamuy et al. 1988) in Figure 5. These fiducial SNEC runs of the BSG merger progenitors yielded underluminous light curves that peaked tens of days later than the observational data, prompting further investigation. For the purposes of this investigation, we define the peak of SN 1987A's light curve as the maximum luminosity following its initial cooling duration (s_1 in Figure 1) and reference minima only after that same feature. The x-axes in our plots are limited to the same time period as the observational data from Hamuy et al. (1988), and the y-axes are limited such that the peak of each light curve is clearly visible.

3.2. *Nickel-56 Variation*

Our first effort to address these discrepancies was to vary the mass of radioactive nickel-56 produced from $0.06M_\odot$ to $0.08M_\odot$ and mix it from the core of the star out to a nickel boundary (defined in mass coordinates), which we also varied from $6M_\odot$ to $8M_\odot$. For these computations, we define a "nickel parameter" equal to the sum of these two values. These data are presented in Figure 7 as a 3x3 grid of plots for all 6 models, though the variations may be better seen on the single plot of model 17-8a in Figure 3. In both figures, we see that the light curves stretch vertically with an increasing nickel mass, resulting in a larger peak luminosity. For each plot in the 3x3 grid, model 16-7b is the least luminous, and model 15-7b is the most luminous.

3.3. *Other Parameters*

In further efforts to increase the luminosity of our light curves, we artificially added energy to one of the progenitors, selecting model 17-8a for its high initial explosion energy (Table 1). Here, we disclude the the gravitational binding energy of the progenitor's outer envelope from our definition of explosion energy, while other works—such as Utrobin et al. (2021)—explicitly include it in their stated explosion energies.

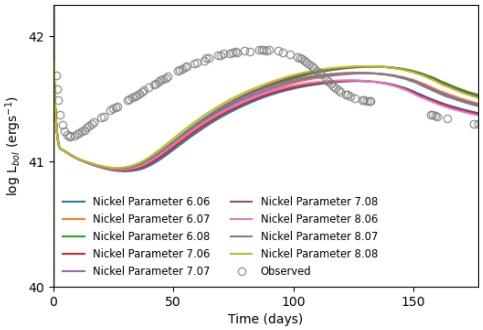

Figure 3. Variant nickel-56 plot for model 17-8a.

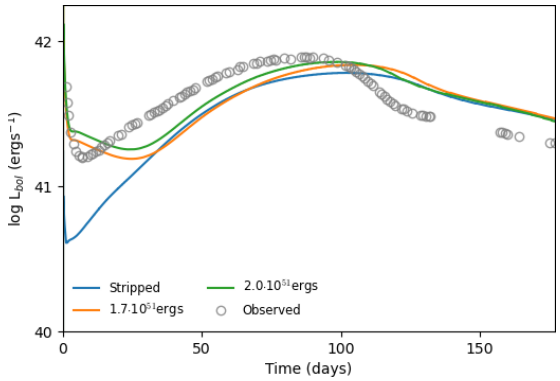

Figure 4. Light curves resulting from varying explosion energy and stripping $\sim 5M_\odot$ from the stellar envelope, as discussed in Section 3.3.

Using SNEC, we added artificial energy up to total explosion energies of $1.7 \cdot 10^{51}$ergs and $2 \cdot 10^{51}$ergs in two separate computations, shown in Figure 4. There is no significant variation between these two light curves, though the more energetic explosion results in a slightly higher peak luminosity. Both still peak later than the observational data (Hamuy et al. 1988). Included on the same plot is a simulation in which we stripped $\sim 5M_\odot$ from the envelope of the 17-8a progenitor, reducing its total mass to $3.704 \cdot 10^{33}$g. The "stripped" run was simulated with the original explosion energy of 17-8a, $1.1 \cdot 10^{51}$ergs, and all three light curves in Figure 4 have a nickel parameter of 8.08. As expected—given that a SN's radiation diffusion time is proportional to its mass—the light curve of the model with a stripped stellar envelope has the lowest peak; however, it has the greatest difference between its minimum and maximum luminosities.

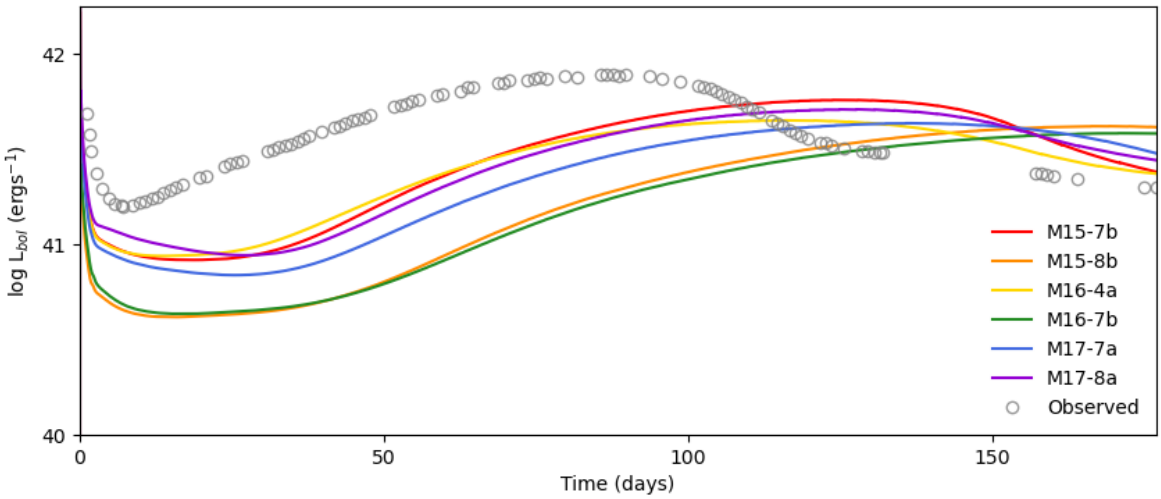

Figure 5. Light curves of each of the un-modified progenitors with a nickel parameter of $5.07M_{\odot}$ and explosion energies listed in Table 1.

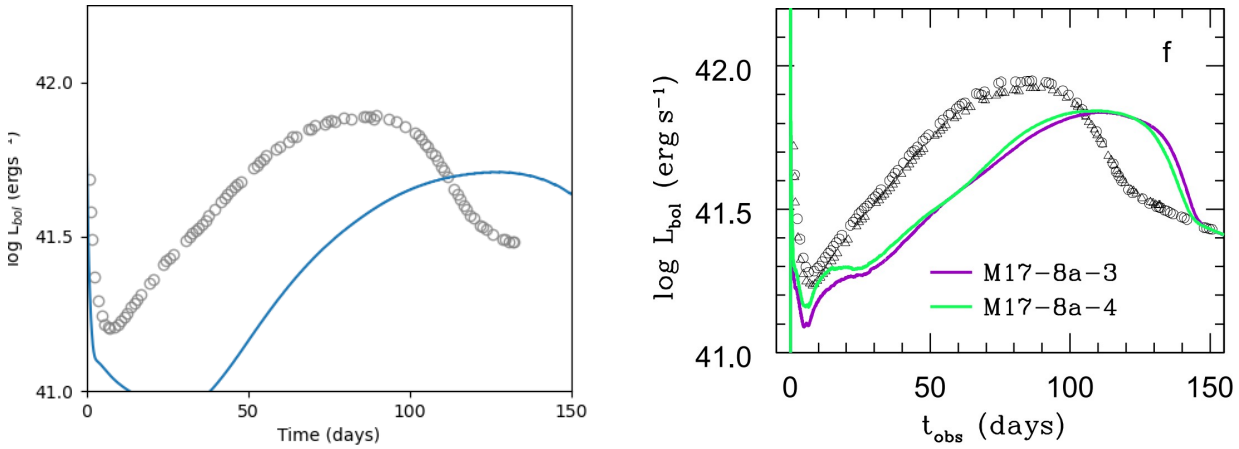

Figure 6. Our light curve output from model 17-8a (left) and those of Utrobin et al. (2021) (right). Both are compared to observational data from Hamuy et al. (1988) in grey, represented by triangles in the plot on the right.

4. DISCUSSION

In the computations for which we varied our defined nickel parameter, we found that the overall nickel mass had a greater impact on the luminosity than the radius from the core to which it is hydrodynamically mixed. This is clearer in Figure 3, where the plots are seen to be grouped by the nickel mass factor of their respective nickel parameters. Of the values we tested, a nickel mass of $0.08M_{\odot}$ resulted in light curves closest to the observational data, confirming that the radioactive decay of nickel-56 plays an active role in determining the maximum luminosity of a SN.

Following the nickel runs, we conclude two initial possibilities. The first and most simple is that STIR may be an inaccurate method for computation, given that all else matches what would be expected of other SN simulations. The discussion becomes more complicated under the assumption that STIR is indeed physically accurate, as expected. Luminosity discrepancies, in this case, could be explained by a proto-magnetar wind. This theory posits that the compact remnant of SN 1987A is a highly-magnetized neutron star, or magnetar, and that the energy it radiated during formation would have added more energy to the SN. It is from that line of reasoning that our artificial energy computations (Figure 4) arose; however, we find the addition of extra explosion energy to have a positive yet insufficient effect on the resultant light curve.

Utrobin et al. (2021) uses explosion energies of $1.075 \cdot 10^{51}$ergs for their run of the modified progenitor 17-8a-3 and $1.216 \cdot 10^{51}$ergs for 17-8a-4, the results of which are compared to our initial run of 17-8a in Figure 6. The variation between definitions of explosion energy between researchers (Section 3.3) explains why our fiducial light curve is under-luminous compared to that of Utrobin et al. (2021). The asymptotic kinetic energies

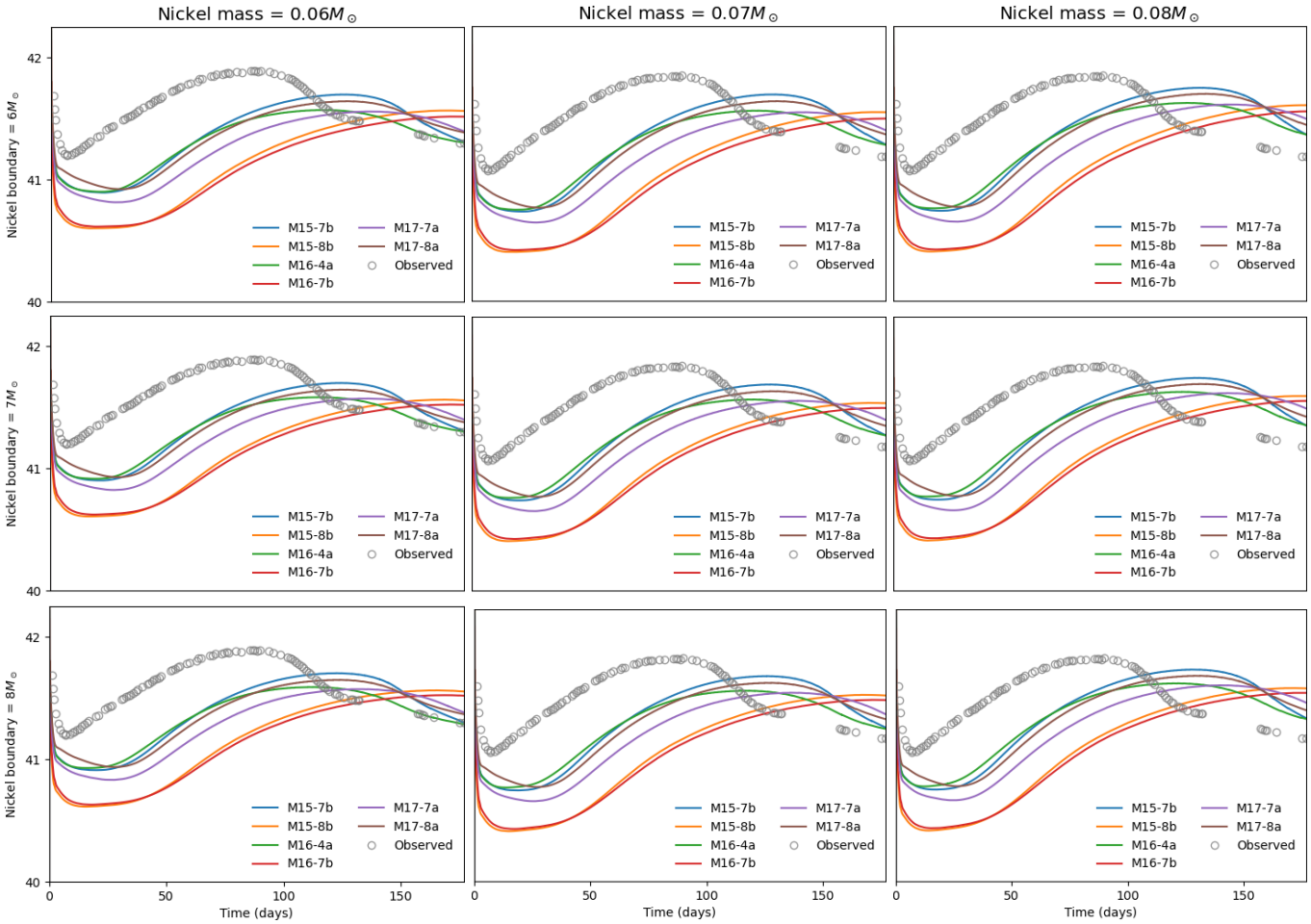

Figure 7. A grid of light curves resulting from varied nickel-56 masses and mixing boundaries.

of the ejecta are lower than our stated explosion energies, since we do not include the gravitational binding energy of the outer envelope in our explosion energy.

A possible explanation for our results continuing to be under-luminous, not addressed by Utrobin et al. (2021), is that the models do not properly account for the angular momentum conserved from the BSG merger. This momentum could be reflected in the resultant progenitor's core, though it is much more likely that it would transfer to the stellar envelope. Angular momentum in the envelope would eject more mass as the star explodes. We took this into consideration by stripping mass from the outer envelope, but found the result less luminous than simply adding artificial explosion energy. Given current understandings of SNe, it makes sense that stripping the envelope off of the progenitor, thus reducing its mass and surface temperature, resulted in less luminous light curves. The stretching may be related to our findings in the nickel variation runs in that reducing the mass of the star from its envelope increases the nickel mass fraction, since the nickel is concentrated near the core.

Regardless, we find that each of our simulation results in Figure 4 for all three runs still differ from when we expect them to peak when hand-calculating from our established parameters. Our interpretation of this is that the typical equations for CCSN dynamics might not apply to the mechanisms which operated SN 1987A, and perhaps Type II Peculiar SNe in general.

5. CONCLUSION

From these data, we preliminarily conclude that BSG merger models with a high nickel mass and explosion energy result in light curves that most resemble that of SN 1987A. Model 17-8a was selected for exploration due to its high initial explosion energy, but that does not rule out the other progenitors. As such, further work will include running the remaining models with explosion energies up to $2 \cdot 10^{51}$ergs and nickel masses of $0.08 M_\odot$. We can also vary the nickel boundaries on models with stripped envelopes to further explore the vertical stretching of their light curves. Given that SN 1987A has associated neutrino observations, these results and those of the proposed future research will be

compared to another study on the neutrino emission rates of these models, providing another angle for narrowing the progenitor parameters and determining the best model through joint analysis of both photon and neutrino emissions.

REFERENCES

Arnett, W. D., Bahcall, J. N., Kirshner, R. P., & Woosley, S. E. 1989, ARA&A, 27, 629, doi: 10.1146/annurev.aa.27.090189.003213

Bethe, H. A., & Wilson, J. R. 1985, ApJ, 295, 14, doi: 10.1086/163343

Bionta, R. M., Blewitt, G., Bratton, C. B., et al. 1987, PhRvL, 58, 1494, doi: 10.1103/PhysRevLett.58.1494

Blanco, W. M., Gregory, B., Hamuy, M., et al. 1987, ApJ, 320, 589, doi: 10.1086/165577

Branch, D., & Wheeler, J. C. 2017, Supernova Explosions, doi: 10.1007/978-3-662-55054-0

Catchpole, R. M., Whitelock, P. A., Feast, M. W., et al. 1988, Monthly Notices of the Royal Astronomical Society, 231, 75P, doi: 10.1093/mnras/231.1.75P

Couch, S. M., & Ott, C. D. 2015, The Astrophysical Journal, 799, 5, doi: 10.1088/0004-637X/799/1/5

Couch, S. M., Warren, M. L., & O'Connor, E. P. 2020, The Astrophysical Journal, 890, 127, doi: 10.3847/1538-4357/ab609e

Gutiérrez, C. P., Anderson, J. P., Hamuy, M., et al. 2017, The Astrophysical Journal, 850, 90, doi: 10.3847/1538-4357/aa8f42

Hamuy, M., Suntzeff, N. B., Gonzalez, R., & Martin, G. 1988, AJ, 95, 63, doi: 10.1086/114613

Hirata, K., Kajita, T., Koshiba, M., et al. 1987, PhRvL, 58, 1490, doi: 10.1103/PhysRevLett.58.1490

McCray, R. 1993, Annual Review of Astronomy and Astrophysics, 31, 175, doi: 10.1146/annurev.aa.31.090193.001135

Menon, A., & Heger, A. 2017, Monthly Notices of the Royal Astronomical Society, 469, 4649, doi: 10.1093/mnras/stx818

Meurer, G., Walborn, N. R., Lasker, B. M., et al. 1987, IAUC, 4321, 2

Minkowski, R. 1941, PASP, 53, 224, doi: 10.1086/125315

Morozova, V., Piro, A. L., Renzo, M., et al. 2015, The Astrophysical Journal, 814, 63, doi: 10.1088/0004-637X/814/1/63

Muijres, L. E. 2010, PhD thesis, Astronomical Institute "Anton Pannekoek", Universiteit van Amsterdam, The Netherlands. https://astro.uni-bonn.de/~nlanger/thesis/lianne.pdf

Nadyozhin, D. K., & Imshennik, V. S. 2005, International Journal of Modern Physics A, 20, 6597, doi: 10.1142/S0217751X05029630

Raffelt, G. G. 2011, Nuclear Physics B - Proceedings Supplements, 221, 218, doi: https://doi.org/10.1016/j.nuclphysbps.2011.09.006

Utrobin, V. P., Wongwathanarat, A., Janka, H.-T., et al. 2021, The Astrophysical Journal, 914, 4, doi: 10.3847/1538-4357/abf4c5

West, R. M., Lauberts, A., Jorgensen, H. E., & Schuster, H. E. 1987, A&A, 177, L1